

Communication

Evaluation of a New Real-Time Dosimeter Sensor for Interventional Radiology Staff

Kenshin Hattori ^{1,†}, Yohei Inaba ^{1,2,†} , Toshiki Kato ¹, Masaki Fujisawa ¹, Hikaru Yasuno ¹, Ayumi Yamada ¹, Yoshihiro Haga ^{1,3}, Masatoshi Suzuki ^{1,2}, Masayuki Zuguchi ¹ and Koichi Chida ^{1,2,*}

¹ Course of Radiological Technology, Health Sciences, Graduate School of Medicine, Tohoku University, 2-1 Seiryō, Aoba-ku, Sendai 980-8575, Japan

² Department of Radiation Disaster Medicine, International Research Institute of Disaster Science, Tohoku University, 468-1 Aramaki Aza-Aoba, Aoba-ku, Sendai 980-0845, Japan

³ Department of Radiology, Sendai Kousei Hospital, 4-5 Hirose-machi, Aoba-ku, Sendai 980-0873, Japan

* Correspondence: chida@med.tohoku.ac.jp; Tel.: +81-22-717-7943

† These authors contributed equally to this work.

Abstract: In 2011, the International Commission on Radiological Protection (ICRP) recommended a significant reduction in the lens-equivalent radiation dose limit, thus from an average of 150 to 20 mSv/year over 5 years. In recent years, the occupational dose has been rising with the increased sophistication of interventional radiology (IVR); management of IVR staff radiation doses has become more important, making real-time radiation monitoring of such staff desirable. Recently, the i3 real-time occupational exposure monitoring system (based on RaySafe™) has replaced the conventional i2 system. Here, we compared the i2 and i3 systems in terms of sensitivity (batch uniformity), tube-voltage dependency, dose linearity, dose-rate dependency, and angle dependency. The sensitivity difference (batch uniformity) was approximately 5%, and the tube-voltage dependency was $<\pm 20\%$ between 50 and 110 kV. Dose linearity was good ($R^2 = 1.00$); a slight dose-rate dependency ($\sim 20\%$) was evident at very high dose rates (250 mGy/h). The i3 dosimeter showed better performance for the lower radiation detection limit compared with the i2 system. The horizontal and vertical angle dependencies of i3 were superior to those of i2. Thus, i3 sensitivity was higher over a wider angle range compared with i2, aiding the measurement of scattered radiation. Unlike the i2 sensor, the influence of backscattered radiation (i.e., radiation from an angle of 180°) was negligible. Therefore, the i3 system may be more appropriate in areas affected by backscatter. In the future, i3 will facilitate real-time dosimetry and dose management during IVR and other applications.

Keywords: radiation protection and safety; fluoroscopy; interventional radiology (IVR); fluoroscopically guided interventional procedures; percutaneous coronary intervention (PCI); eye lens dose; occupational radiation exposure; X-ray examination; real-time radiation sensor



Citation: Hattori, K.; Inaba, Y.; Kato, T.; Fujisawa, M.; Yasuno, H.; Yamada, A.; Haga, Y.; Suzuki, M.; Zuguchi, M.; Chida, K. Evaluation of a New Real-Time Dosimeter Sensor for Interventional Radiology Staff. *Sensors* **2023**, *23*, 512. <https://doi.org/10.3390/s23010512>

Academic Editor: Flavio Esposito

Received: 11 November 2022

Revised: 20 December 2022

Accepted: 28 December 2022

Published: 3 January 2023



Copyright: © 2023 by the authors. Licensee MDPI, Basel, Switzerland. This article is an open access article distributed under the terms and conditions of the Creative Commons Attribution (CC BY) license (<https://creativecommons.org/licenses/by/4.0/>).

1. Introduction

Medical radiation (patient radiation doses and occupational exposure) is a major problem in radiation medicine [1–10].

Interventional radiology (IVR) plays a major role in disease diagnosis and treatment. IVR is performed using X-ray imaging equipment, catheters, and needles [11–14].

The procedural times of sophisticated IVR and other procedures have lengthened, increasing the radiation dose and making radiation control very important [15–22].

The 2011 statement of the International Commission on Radiological Protection (ICRP) reduced the eye-lens exposure limit (the occupational dose) from 150 to 20 mSv/year [23]. It is expected that some medical staff will exceed this, and thus it is essential to evaluate the dose to the lens. Currently, in Japan, radiation doses delivered to medical staff during IVR and other procedures are assessed principally using radiation-monitoring badges attached to the neck, chest, or abdomen. Such badges measure cumulative doses over a long period

(e.g., 1 month), not the dose associated with each examination or procedure. We think that it may be difficult to reduce the occupational dose further in the absence of real-time radiation monitoring in IVR. Originally, the RaySafe i2 (i2) real-time dosimeter was used (Figure 1a). This has been replaced by the RaySafe i3 (i3) (Figure 1b) [24,25]. According to the manufacturer, the i3 is better than the i2 in terms of scattered-radiation detection, easy battery replacement, and analytical performance. Here, we compared the i3 and i2 dosimeters (sensors) [26].



Figure 1. (a) The RaySafe i2 sensor (44 × 45 mm); (b) The RaySafe i3 sensor (40 × 58 mm). Recently, the i3 sensor has replaced the former i2 sensor.

2. Materials and Methods

2.1. The i3 Dosimeter

Like the i2 dosimeter, the i3 measures scattered radiation (1 cm dose equivalent) in real-time, displaying both the dose rate and the cumulative dose (Figure 2). The dose rate is displayed as a red, yellow, or green bar, from the highest to the lowest dose, that is refreshed at 1-s intervals; a glance is sufficient to determine whether the dose rate is high. The i3 system stores dose data; a chronological dose history can be viewed and subjected to time-series analysis using a PC running dedicated software. Additionally, the i3 dosimeter uses a replaceable battery as opposed to the i2 dosimeter model in which the battery is non-replaceable.



Figure 2. A schematic of the i3 system (left: base station with 10.4-inch display; right: i3 dosimeter sensor). The system comprises a wireless i3 sensor (solid-state semiconductor detector) that transmits the scattered-radiation dose to the base station. The i3 sensor is small (40 × 58 mm, 34 g) and thus easy to carry during interventions.

2.2. Fundamental Evaluation

We used a diagnostic X-ray system featuring a high-frequency inverter generator (DHF-155H, Hitachi) to evaluate the i3 system. The total filtration of this X-ray system was 3.6-mm-aluminum equivalent. The distance from the X-ray tube to the i3 system was 180 cm, and the exposed area (the radiation-field size) at the i3 entrance was 30×30 cm. Variation in the sensitivity (batch uniformity) of i3 systems was evaluated by directly irradiating four i3 systems and an ionization chamber dosimeter simultaneously (Figure 3). Fluoroscopy was performed for 1 min under three conditions: (1) 65 kV tube voltage and 1 mA tube current, (2) 65 kV tube voltage and 0.1 mA tube current, and (3) 40 kV tube voltage and 0.1 mA tube current. These X-ray output conditions were to simulate scattered radiation (i.e., a low dose rate). To confirm reproducibility, all measurements were performed 10 times. An ionization chamber calibrated using the Japan national standard exposure dose (thimble type 6 mL; Model-9015, Radcal) was used to confirm the stability of the instrument.

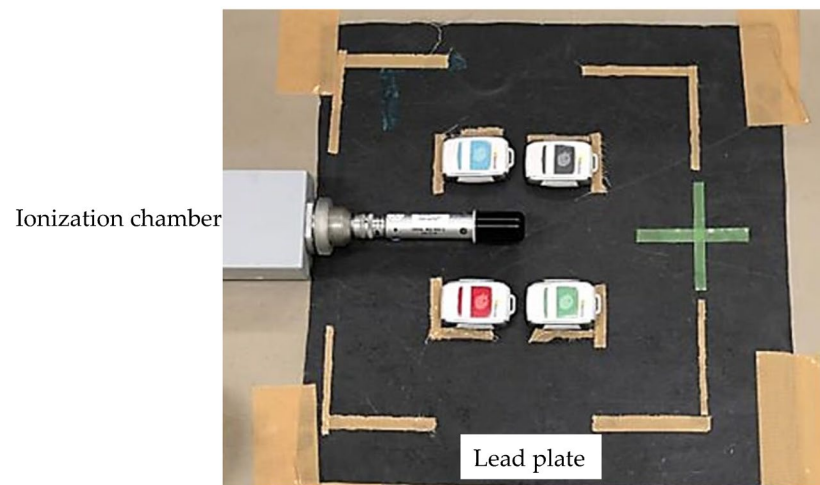


Figure 3. Experimental layout. The exposed area (radiation field) at the i3 entrance was 30×30 cm.

The tube-voltage dependency of the i3 system was evaluated under the same geometric conditions as employed when assessing batch uniformity. Fluoroscopy was continuous over 1 min, as shown in Table 1. Three measurements were made at each tube voltage, and the averages were calculated. The tube-voltage dependency for the i3 dosimeter was the ratio of the average i3 value to that of the ionization chamber dosimeter.

Table 1. Fluoroscopic X-ray tube voltage and half value layer.

Tube Voltage (kV)	50	60	70	80	90	100	110
Half value layer (mmAl)	2.0	2.4	2.8	3.2	3.7	4.15	4.7

Dose linearity was measured using the integrated dose for X-ray irradiation of the four i3 systems under the same geometric conditions employed to evaluate batch uniformity. The fluoroscopy conditions were a 65 kV tube voltage, 1.6 mA tube current, and 15 min fluoroscopy time. The i3 integrated doses were recorded at 1, 2, 4, 6, 8, 10, 12, 14, and 15 min after fluoroscopy commencement. The experiment was repeated three times. For each dataset, the coefficient of determination (R^2) was calculated by approximating linearity using the least-squares method in Microsoft Excel.

The dose-rate dependency of the i3 system was measured at 11 different dose rates ranging from 20–500 mGy/h. The dose-rate dependency was the ratio of the mean i3 value to that of the ionization chamber dosimeter. Copper plates were attached to the X-ray tube

entrance when measuring low dose rates. The i2 dosimeter was evaluated under the same conditions, and the dose-rate dependencies of the i2 and i3 systems were compared.

The limit of radiation detection of the i2 and i3 systems was evaluated using fluoroscopy scatter radiation from an acrylic phantom. The fluoroscopy tube voltages were 60, 80, and 100 kV, and the fluoroscopy durations were 3, 10, and 60 s.

A digital cine single-plane X-ray system (Infinix Celeve-I: INF8000F, Toshiba Medical) was used to measure angle dependency. The i3 sensor was placed 75 cm from the focal point of the X-ray tube and irradiated in free air. The dependency of the i3 sensor on the X-ray beam angle in air was measured at 0° , $\pm 15^\circ$, $\pm 30^\circ$, $\pm 45^\circ$, $\pm 60^\circ$, $\pm 75^\circ$, $\pm 90^\circ$, $\pm 135^\circ$, and 180° along the vertical and horizontal axes under identical X-ray conditions (70 kV, HVL, 2.7 mm aluminum, 10 mA, 5 ms); the 0° measurement served as the reference value. The experiment was repeated five times at each angle (Figure 4). This method is that of Inaba et al. [26].

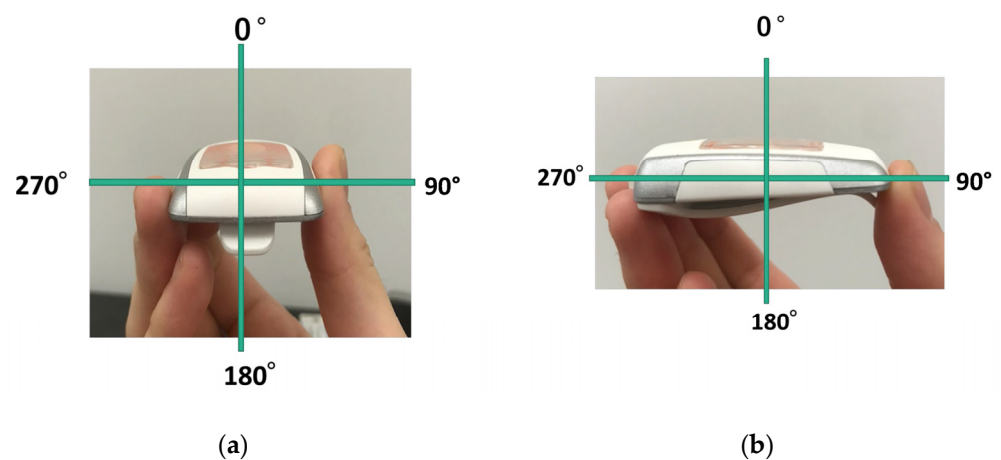


Figure 4. Experimental layout for evaluation of angle dependency: (a) Horizontal; (b) Vertical.

3. Results

3.1. Fundamental Evaluation

Table 2 shows the variations in sensitivity (batch uniformity). For the first condition, the reproducibility of each detector (average coefficient of variation (CV), $CV = \text{standard deviation} / \text{mean measurements}$) was 2.099% (range 1.380–3.192%), and the batch uniformity (CV of each i3 sensor measurement) was 3.239%. For the second condition, the reproducibility of each detector was 2.216% (range 1.934–2.398%) and the batch uniformity was 3.431%. For the third condition, the reproducibility of each detector was 4.847% (range 2.291–6.913%) and the batch uniformity was 8.141%.

Table 2. Variations in sensitivity (reproducibility, batch uniformity).

	Reproducibility (%)	Batch Uniformity (%)
condition (1)	2.099 (range 1.380–3.192)	3.24
condition (2)	2.216 (range 1.934–2.398)	3.43
condition (3)	4.847 (range 2.291–6.913)	8.14

Figure 5 shows the i3 tube-voltage dependency with respect to that of the ionization chamber dosimeter. Although the i3 value decreased with decreasing tube voltage, the difference in the i3 and chamber dosimeter values was $< \pm 20\%$, using the 70 kV measurement as the reference value.

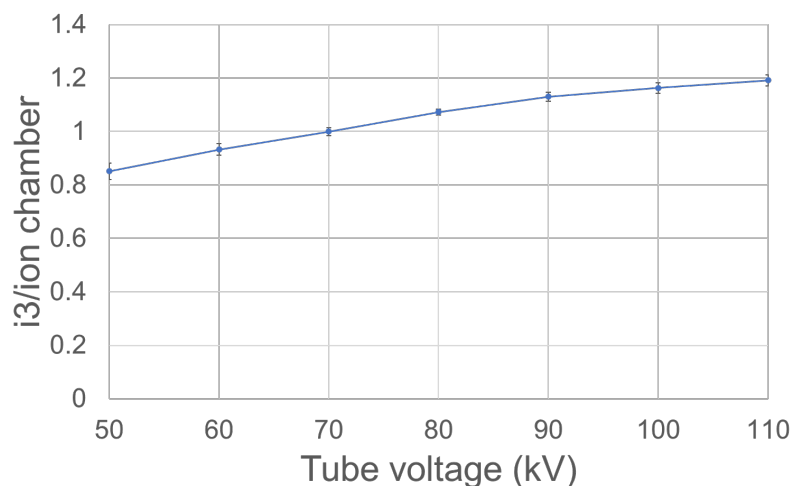


Figure 5. Tube-voltage dependencies of the i3 system (vertical axis: i3 measurements/ionization chamber measurements; horizontal axis: tube voltage).

Figure 6 shows the dose linearities. The R^2 was 1.00.

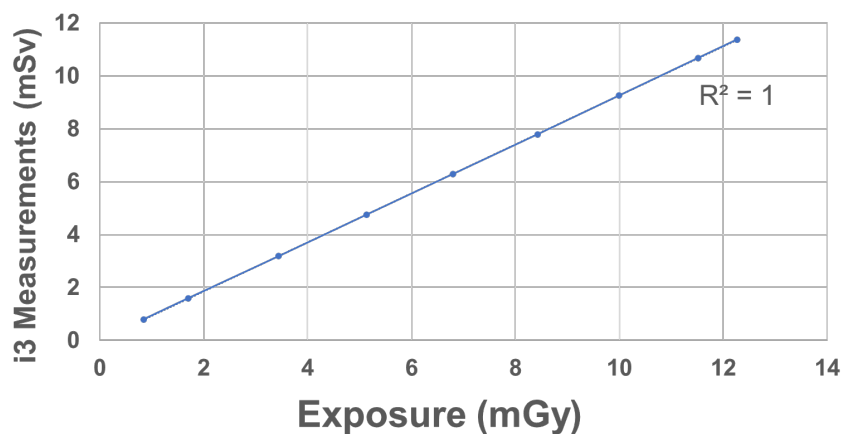


Figure 6. Dose linearities of the i3 system (vertical axis: i3 measurements; horizontal axis: ionization-chamber measurements).

Figure 7 shows the dose-rate dependencies. The dose per hour is shown on the horizontal axis, and the ionization-chamber dosimeter reading divided by those of the i2 or i3 is shown on the vertical axis. At low dose rates, the i2 and i3 responses were similar. At very high dose rates (250 mGy/h), both the i2 and i3 evidenced dose-rate dependency (~20%).

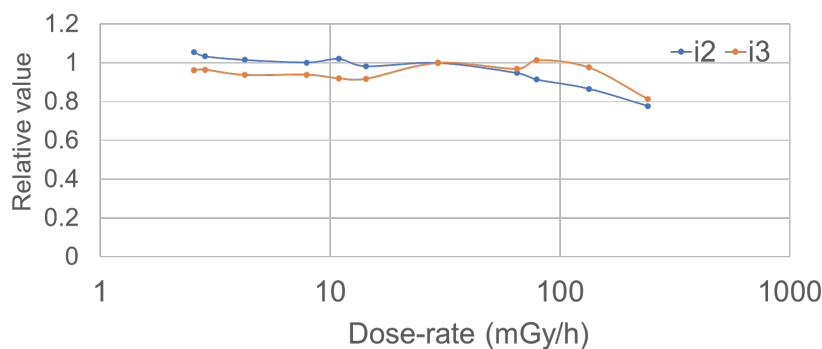


Figure 7. Dose-rate dependencies (vertical axis: i3 or i2 measurements/ionization-chamber measurements; horizontal axis: ionization-chamber measurements).

Table 3 shows the limit of radiation detection of the i3 and i2 dosimeters. The i3 dosimeter showed better performance for the lower radiation detection limit compared with the i2 system.

Table 3. Low radiation detection limit of the i2 and i3 systems.

Tube Voltage	60 kV			80 kV			100 kV			
	Fluoroscopy Duration	3 s	10 s	60 s	3 s	10 s	60 s	3 s	10 s	60 s
i3 measurements ($\mu\text{Sv/h}$)		57.5	30.5	19.5	59.6	34.5	21.3	48.4	27.3	16.6
i2 measurements ($\mu\text{Sv/h}$)		185.7	46.3	41.3	101.3	31.2	35.2	99.8	39.8	22.2

3.2. Angle Dependency

Figure 8a,b show the results in the horizontal and vertical directions, respectively. All doses are expressed as relative values, where 1 is the dose at 0° . In the horizontal direction, the i3 exhibited a reliable dose response from 0 to $\pm 75^\circ$ with a sensitivity $>80\%$. In the vertical direction, the i3 exhibited a reliable dose response from 0 to $+65^\circ$ and 0 to $+270^\circ$ (-90°) with a sensitivity $>80\%$. Figure 9a,b show the i2 sensitivities in the horizontal and vertical directions, respectively. i3 evidenced better angle dependency than that of i2. Furthermore, using the i2 sensor, the influence of backscattered radiation must be considered.

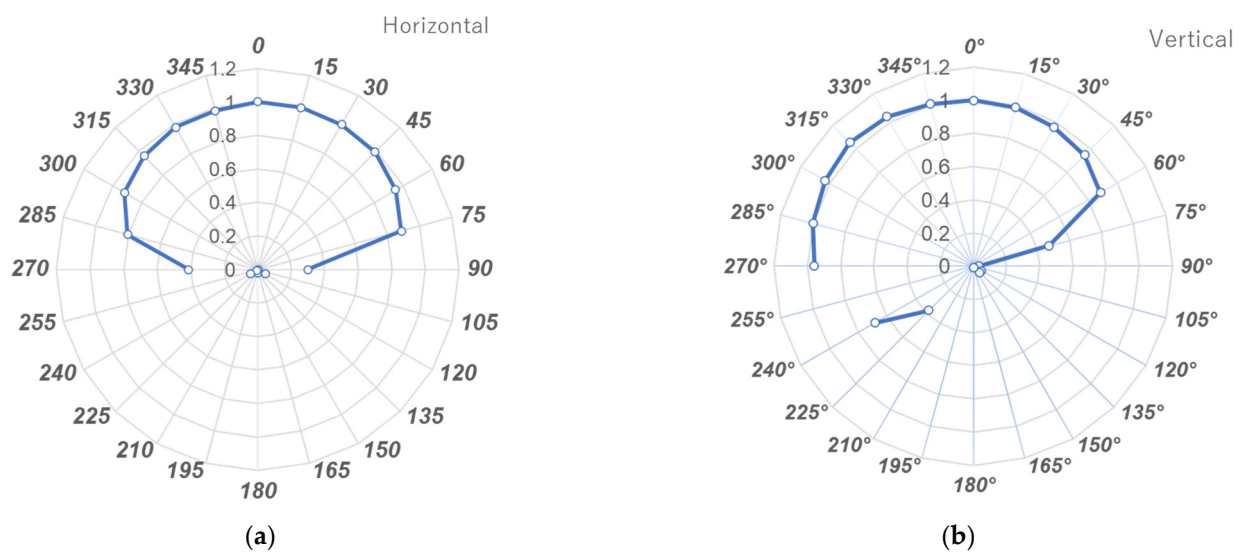


Figure 8. Angle dependency of the i3 sensor: (a) Horizontal plane; (b) Vertical plane.

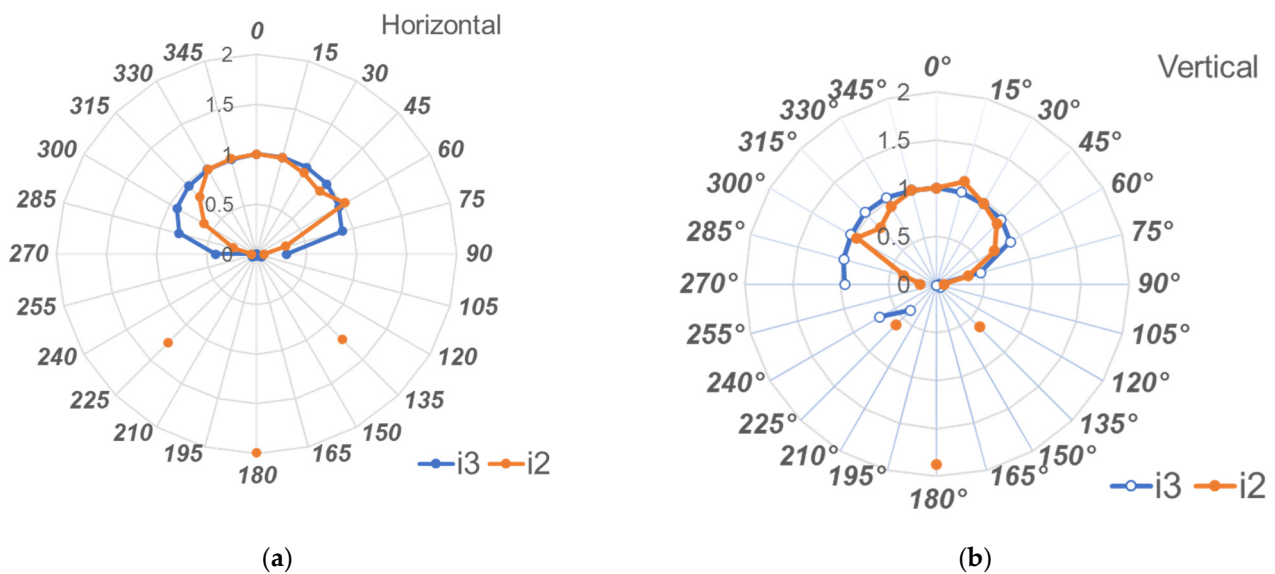


Figure 9. Angle dependencies of the i3 and i2 sensors: (a) Horizontal plane; (b) Vertical plane.

4. Discussion

Safety measures to prevent radiation exposure are important due to the risk of radiation-induced injuries, such as skin damage in patients and cataracts in medical staff [27–37]. Therefore, increasing attention is being paid to radiation safety and protection for patients and medical staff, particularly related to IVR [38–47].

Radiation monitoring badges (e.g., glass badges) and pocket dosimeters are used extensively to assess radiation doses to medical staff. Glass badges measure long-term exposure, but they cannot be used for real-time measurements. Pocket dosimeters measure doses in real-time, but must be constantly checked. Unlike the i3 system, pocket dosimeters do not display doses in real-time on a monitor. Dosimeters placed in the vicinity of the lens, such as the Eye-D and DOSIRIS, can also be used [26,48–52]; the passive DOSIRIS dosimeter, which does not provide real-time monitoring, was designed to measure the lens dose, but the real-time i3 system may be more effective for reducing occupational doses. The use of dosimeters such as the i3 will be valuable in situations such as IVR, in which exposure doses are high and instantaneous monitoring is required [53–58].

Real-time monitoring is important to minimize the exposure of medical staff and to ensure adequate protection [59–64]. To the best of our knowledge, this is the first detailed fundamental study of the ability of the i3 dosimeter to monitor the real-time occupational doses of IVR staff. The reproducibility of each i3 system and the batch uniformity among the systems were both approximately 5%, thus comparable with or better than those of the i2 system.

In terms of tube-voltage dependency, the lower the tube voltage, the slightly lower the i3 value. However, if the ratio of the values measured at 70 kV was set to 1, the difference between the 50 and 110 kV values was $<\pm 20\%$, thus well within the $\pm 25\%$ range of the Raysafe instruction manual [25].

The dose linearity of the i3 system was good ($R^2 = 1$). It was reported previously (Inaba [26]) that the i2 dose linearity is also good ($R^2 = 1$). The i2 and i3 systems may be similar in this respect.

In terms of the dose-rate dependency, a decrease in sensitivity was observed at high dose rates (e.g., 250 mGy/h) for both dosimeters. As the scattered radiation received by an IVR physician is lower than this, we do not perceive a clinical problem. In detail, the diagnostic reference level (DRL) of the patient reference fluoroscopy dose rate during IVR in Japan (Japan DRL2020 [65]) is 17 mGy/min (i.e., 102 mGy/h). An IVR physician may receive between 1/1000 and 1/500 of the patient entrance dose, so, it has been thought that IVR physicians are not exposed to high dose rates (e.g., 250 mGy/h).

The angle dependency of the i3 system was good in both the horizontal (0 to $\pm 75^\circ$) and vertical (0° to $+65^\circ$ and -90°) axes. The angle dependency of the i3 was better than that of the i2. Regarding the semiconductor sensor and the internal structure of the dosimeter, there is no detailed information disclosure from the manufacturer. Figure 10 shows X-ray photographs from the i3 and i2 dosimeters. We speculate that the X-ray sensor of the i3 dosimeter has improved angle dependency by being placed at the bottom of the sensor compared to the i2 dosimeter in which the sensor is located at the upper right side.

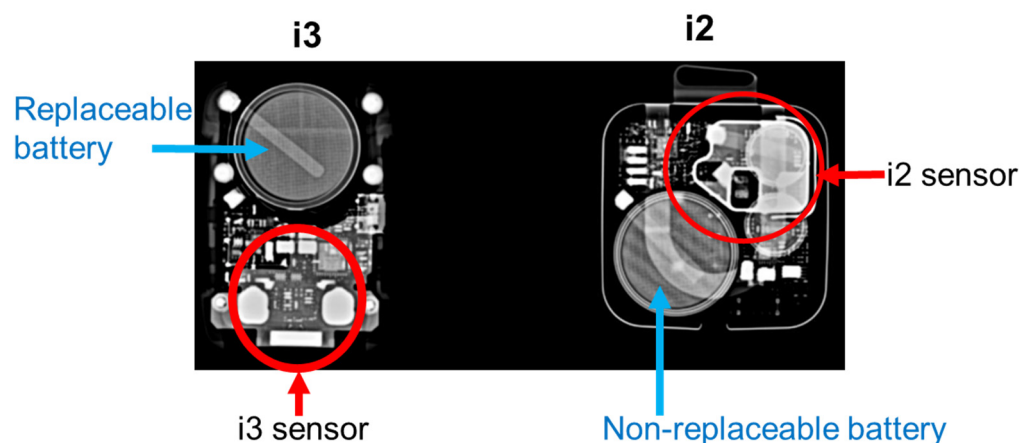


Figure 10. X-ray photographs for the i3 and i2 dosimeters.

Behind the sensor, i2 sensitivity almost doubled, whereas i3 was insensitive. When a dosimeter is mounted on the head or neck, backscattering must be considered. As the i3 is insensitive behind the sensor, such effects can be ignored.

The basic performance of the i3 system was thus equal to or better than that of the i2 system; the i3 should be preferred by medical staff. Although pocket dosimeters can measure doses in real-time, the i3 dosimeter is better because a glance at the display reveals the current dose, increasing radiation awareness.

In summary, the dose limits for medical personnel have been reduced in many countries; in Japan, the dose limit was significantly reduced from 150 to an average of 20 mSv/year over a 5-year period. Personal dose management is becoming increasingly important. Currently, badges (e.g., glass badges) and pocket dosimeters are used by medical staff; in the future, real-time dosimeters may become more important, especially in IVR. We previously reported the basic performance of the former i2 system (i2 sensor). Recently, a new i3 dosimeter (sensor) was developed to replace the i2 sensor. Here, we evaluated the basic performance of the new sensor (i3 system). The results show that the basic performance of the new i3 sensor is the same as or better than that of the i2 sensor. To date, it has not been possible to determine the chronological dose history (e.g., the dose rate, and exposure duration); the i3 system enables history determination at a glance. The i3 dosimeter is appropriate for clinical use, exhibiting especially good angle dependency. Such dosimeters will remain important in the future.

5. Conclusions

The i3 dosimeter performs as well as, or better than, the i2 dosimeter. The angle dependency of the i3 is particularly good. Furthermore, unlike the i2, the i3 can be used in areas exposed to backscatter. In the future, i3 will facilitate real-time dosimetry and dose management during IVR and other applications.

Author Contributions: Conceptualization, Y.I., M.Z. and K.C.; methodology, Y.H., Y.I. and K.C.; software, K.H., Y.H. and M.S.; validation, K.H., Y.I., M.S., M.Z. and K.C.; formal analysis, K.H., T.K., M.F., H.Y., A.Y., Y.I., M.S. and K.C.; investigation, K.H., T.K., M.F., H.Y., A.Y. and K.C.; resources, Y.H., Y.I. and K.C.; data curation, K.H., T.K., M.F., H.Y., A.Y., Y.I. and M.S.; writing—original draft preparation, K.H., T.K., M.F., H.Y., A.Y. and K.C.; writing—review and editing, K.H., M.Z., Y.I., M.S.

and K.C.; visualization, K.H., Y.I. and M.S.; supervision, Y.H., M.Z. and K.C.; project administration, Y.I., M.Z. and K.C.; funding acquisition, K.C. All authors have read and agreed to the published version of the manuscript.

Funding: This study was supported in part by the Industrial Disease Clinical Research Grants (200701-1), Japan.

Institutional Review Board Statement: “Not applicable” for studies not involving humans or animals.

Informed Consent Statement: Not applicable.

Data Availability Statement: Not applicable.

Acknowledgments: We would like to express our deepest gratitude to Masahiro Sota, Mitsuya Abe and Yuji Kaga of the Sendai Kosei Hospital for their assistance with the study.

Conflicts of Interest: The authors declare no conflict of interest.

References

1. Vano, E.; Escaned, J.; Vano-Galvan, S.; Fernandez, J.M.; Galvan, C. Importance of a patient dosimetry and clinical followup program in the detection of radiodermatitis after long percutaneous coronary interventions. *Cardiovasc. Intervent. Radiol.* **2013**, *36*, 330–337. [CrossRef] [PubMed]
2. Chida, K.; Inaba, Y.; Masuyama, H.; Yanagawa, I.; Mori, I.; Saito, H.; Maruoka, S.; Zuguchi, M. Evaluating the performance of a MOSFET dosimeter at diagnostic X-ray energies for interventional radiology. *Radiol. Phys. Technol.* **2009**, *2*, 58–61. [CrossRef] [PubMed]
3. Matsunaga, Y.; Haba, T.; Kobayashi, M.; Suzuki, S.; Asada, Y.; Chida, K. Novel pregnant model phantoms for measurement of foetal radiation dose in x-ray examinations. *J. Radiol. Prot.* **2021**, *41*, N12–N21. [CrossRef] [PubMed]
4. Inaba, Y.; Chida, K.; Kobayashi, R.; Zuguchi, M. A cross-sectional study of the radiation dose and image quality of X-ray equipment used in IVR. *J. Appl. Clin. Med. Phys.* **2016**, *17*, 91–401. [CrossRef] [PubMed]
5. Chida, K.; Ohno, T.; Kakizaki, S.; Takegawa, M.; Yuuki, H.; Nakada, M.; Takahashi, S.; Zuguchi, M. Radiation dose to the pediatric cardiac catheterization and intervention patient. *Am. J. Roentgenol.* **2010**, *195*, 1175–1179. [CrossRef]
6. Nemoto, M.; Chida, K. Reducing the breast cancer risk and radiation dose of radiography for scoliosis in children: A phantom study. *Diagnostics* **2020**, *10*, 753. [CrossRef]
7. Chida, K.; Saito, H.; Otani, H.; Kohzuki, M.; Takahashi, S.; Yamada, S.; Shirato, K.; Zuguchi, M. Relationship between fluoroscopic time, dose—Area product, body weight, and maximum radiation skin dose in cardiac interventional procedures. *Am. J. Roentgenol.* **2006**, *186*, 774–778. [CrossRef]
8. Inaba, Y.; Nakamura, M.; Zuguchi, M.; Chida, K. Development of novel real-time radiation systems using 4-channel sensors. *Sensors* **2020**, *20*, 2741. [CrossRef]
9. Matsuzaki, S.; Moritake, T.; Morota, K.; Nagamoto, K.; Nakagami, K.; Kuriyama, T.; Kunugita, N. Development and assessment of an educational application for the proper use of ceiling-suspended radiation shielding screens in angiography rooms using augmented reality technology. *Eur. J. Radiol.* **2021**, *143*, 109925. [CrossRef]
10. Sato, T.; Eguchi, Y.; Yamazaki, C.; Hino, T.; Saida, T.; Chida, K. Development of a New Radiation Shield for the Face and Neck of IVR Physicians. *Bioengineering* **2022**, *9*, 354. [CrossRef]
11. International Commission on Radiological Protection (ICRP). *Radiological Protection in Cardiology*; ICRP Publication 120; Elsevier: Amsterdam, The Netherlands, 2013; Volume 42, Available online: https://journals.sagepub.com/doi/pdf/10.1177/ANIB_42_1 (accessed on 1 November 2022).
12. Chida, K.; Kato, M.; Kagaya, Y.; Zuguchi, M.; Saito, H.; Ishibashi, T.; Takahashi, S.; Yamada, S.; Takai, Y. Radiation dose and radiation protection for patients and physicians during interventional procedure. *J. Radiat. Res.* **2010**, *51*, 97–105. [CrossRef]
13. Haga, Y.; Chida, K.; Sota, M.; Kaga, Y.; Abe, M.; Inaba, Y.; Suzuki, M.; Meguro, T.; Zuguchi, M. Hybrid operating room system for the treatment of thoracic and abdominal aortic aneurysms: Evaluation of the radiation dose received by patients. *Diagnostics* **2020**, *10*, 846. [CrossRef]
14. Chida, K. What are useful methods to reduce occupational radiation exposure among radiological medical workers, especially for interventional radiology personnel? *Radiol. Phys. Technol.* **2022**, *15*, 101–115. [CrossRef]
15. Vañó, E.; Gonzalez, L.; Fernández, J.M.; Haskal, Z.J. Eye lens exposure to radiation in interventional suites: Caution is warranted. *Radiology* **2008**, *248*, 945–953. [CrossRef]
16. Kato, M.; Chida, K.; Sato, T.; Oosaka, H.; Tosa, T.; Kadowaki, K. Evaluating the maximum patient radiation dose in cardiac interventional procedures. *Radiat. Prot. Dosim.* **2011**, *143*, 69–73. [CrossRef]
17. Inaba, Y.; Chida, K.; Shirotori, K.; Shimura, H.; Yanagawa, I.; Zuguchi, M.; Takahashi, S. Comparison of the radiation dose in a cardiac IVR X-ray system. *Radiat. Prot. Dosim.* **2011**, *143*, 74–80. [CrossRef]

18. International Commission on Radiological Protection (ICRP). *ICRP Statement on Tissue Reactions/Early and Late Effects of Radiation in Normal Tissues and Organs, Threshold Doses for Tissue Reactions in a Radiation Protection Context*; ICRP publication 118 Ann. Elsevier: Amsterdam, The Netherlands, 2012; Volume 41, pp. 1–322. Available online: <https://www.icrp.org/publication.asp?id=ICRP%20Publication%20118> (accessed on 1 November 2022).
19. Chida, K.; Morishima, Y.; Inaba, Y.; Taura, M.; Ebata, A.; Takeda, K.; Shimura, H.; Zuguchi, M. Physician-received scatter radiation with angiography systems used for interventional radiology: Comparison among many X-ray systems. *Radiat. Prot. Dosim.* **2011**, *149*, 410–416. [[CrossRef](#)]
20. Zuguchi, M.; Chida, K.; Taura, M.; Inaba, Y.; Ebata, A.; Yamada, S. Usefulness of non-lead aprons in radiation protection for physicians performing interventional procedures. *Radiat. Prot. Dosim.* **2008**, *131*, 531–534. [[CrossRef](#)]
21. Ishii, H.; Chida, K.; Satsurai, K.; Haga, Y.; Kaga, Y.; Abe, M.; Inaba, Y.; Zuguchi, M. Occupational eye dose correlation with neck dose and patient-related quantities in interventional cardiology procedures. *Radiol. Phys. Technol.* **2021**, *15*, 54–62. [[CrossRef](#)]
22. Chida, K.; Takahashi, T.; Ito, D.; Shimura, H.; Takeda, K.; Zuguchi, M. Clarifying and visualizing sources of staff-received scattered radiation in interventional procedures. *Am. J. Roentgenol.* **2011**, *197*, W900–W903. [[CrossRef](#)]
23. International Commission on Radiological Protection (ICRP). *Statement on Tissue Reactions*; Elsevier: Amsterdam, The Netherlands, 2011. Available online: <http://www.icrp.org/docs/ICRP%20Statement%20on%20Tissue%20Reactions.pdf> (accessed on 1 November 2022).
24. RaySafe i3 Real-Time Radiation Dosimeter | RaySafe. Available online: <https://www.raysafe.com/products/real-time-staff-dosimetry/raysafe-i3-real-time-radiation-dosimeter> (accessed on 1 November 2022).
25. RaySafe i3. Available online: <https://www.raysafe.com/sites/default/files/2020-07/RaySafe%20i3%20OSD%20Instructions%20for%20Use%20%28multilingual%29.pdf> (accessed on 1 November 2022).
26. Inaba, Y.; Chida, K.; Kobayashi, R.; Kaga, Y.; Zuguchi, M. Fundamental study of a real-time occupational dosimetry system for interventional radiology staff. *J. Radiol. Prot.* **2014**, *34*, 65–71. [[CrossRef](#)] [[PubMed](#)]
27. Coppeta, L.; Pietroiusti, A.; Neri, A.; Spataro, A.; Angelis, E.D.; Perrone, S.; Magrini, A. Risk of radiation-induced lens opacities among surgeons and interventional medical staff. *Radiol. Phys. Technol.* **2019**, *12*, 26–29. [[CrossRef](#)] [[PubMed](#)]
28. Magee, J.S.; Martin, C.J.; Sandblom, V.; Carter, M.J.; Almén, A.; Cederblad, Å.; Jonasson, P.; Lundh, C. Derivation and application of dose reduction factors for protective eyewear worn in interventional radiology and cardiology. *J. Radiol. Prot.* **2014**, *34*, 811–823. [[CrossRef](#)] [[PubMed](#)]
29. Omar, A.; Kadesjö, N.; Palmgren, C.; Marteinsdottir, M.; Segerdahl, T.; Fransson, A. Assessment of the occupational eye lens dose for clinical staff in interventional radiology, cardiology and neuroradiology. *J. Radiol. Prot.* **2017**, *37*, 145–159. [[CrossRef](#)] [[PubMed](#)]
30. Božović, P.; Ciraj-Bjelac, O.; Petrović, J.S. Occupational eye lens dose estimated using whole—Body dosimeter in interventional cardiology and radiology: A Monte Carlo study. *Radiat. Prot. Dosim.* **2019**, *185*, 135–142. [[CrossRef](#)]
31. Kato, M.; Chida, K.; Sato, T.; Oosaka, H.; Tosa, T.; Munehisa, M.; Kadowaki, K. The necessity of follow-up for radiation skin injuries in patients after percutaneous coronary interventions: Radiation skin injuries will often be overlooked clinically. *Acta Radiol.* **2012**, *53*, 1040–1044. [[CrossRef](#)]
32. Vaňo, E.; González, L.; Beneytez, F.; Moreno, F. Lens injuries induced by occupational exposure in non-optimized interventional radiology laboratories. *Br. J. Radiol.* **1998**, *71*, 728–733. [[CrossRef](#)]
33. Vigneux, G.; Pirkkanen, J.; Laframboise, T.; Prescott, H.; Tharmalingam, S.; Thome, C. Radiation-Induced Alterations in Proliferation, Migration, and Adhesion in Lens Epithelial Cells and Implications for Cataract Development. *Bioengineering* **2022**, *9*, 29. [[CrossRef](#)]
34. Chida, K.; Kaga, Y.; Haga, Y.; Kataoka, N.; Kumasaka, E.; Meguro, T.; Zuguchi, M. Occupational dose in interventional radiology procedures. *Am. J. Roentgenol.* **2013**, *200*, 138–141. [[CrossRef](#)]
35. Chida, K.; Morishima, Y.; Masuyama, H.; Chiba, H.; Katahira, Y.; Inaba, Y.; Mori, I.; Maruoka, S.; Takahashi, S.; Kohzuki, M.; et al. Effect of radiation monitoring method and formula differences on estimated physician dose during percutaneous coronary intervention. *Acta Radiol.* **2009**, *50*, 170–173. [[CrossRef](#)]
36. Koenig, A.; Maas, J.; Viniol, S.; Etzel, R.; Fiebich, M.; Thomas, R.; Mahnken, A. Scatter radiation reduction with a radiation-absorbing pad in interventional radiology examinations. *Eur. J. Radiol.* **2020**, *132*, 109245. [[CrossRef](#)]
37. Yokoyama, S.; Suzuki, S.; Toyama, H.; Arakawa, S.; Inoue, S.; Kinomura, Y.; Kobayashi, I. Evaluation of eye lens dose of interventional cardiologists. *Radiat. Prot. Dosim.* **2017**, *173*, 218–222. [[CrossRef](#)]
38. Morishima, Y.; Chida, K.; Katahira, Y. The effectiveness of additional lead-shielding drape and low pulse rate fluoroscopy in protecting staff from scatter radiation during cardiac resynchronization therapy (CRT). *Jpn. J. Radiol.* **2019**, *37*, 95–101. [[CrossRef](#)]
39. Inaba, Y.; Chida, K.; Murabayashi, Y.; Endo, M.; Otomo, K.; Zuguchi, M. An initial investigation of a wireless patient radiation dosimeter for use in interventional radiology. *Radiol. Phys. Technol.* **2020**, *13*, 321–326. [[CrossRef](#)]
40. Morishima, Y.; Chida, K.; Meguro, T.; Hirota, M.; Chiba, H.; Fukuda, H. Lens equivalent dose of staff during endoscopic retrograde cholangiopancreatography: Dose comparison using two types of dosimeters. *Radiat. Prot. Dosim.* **2022**, *198*, 1368–1376. [[CrossRef](#)]
41. Matsunaga, Y.; Chida, K.; Kondo, Y.; Kobayashi, K.; Kobayashi, M.; Minami, K.; Suzuki, S.; Asada, Y. Diagnostic reference levels and achievable doses for common computed tomography examinations: Results from the Japanese nationwide dose survey. *Br. J. Radiol.* **2019**, *92*, 20180290. [[CrossRef](#)]

42. Endo, M.; Haga, Y.; Sota, M.; Tanaka, A.; Otomo, K.; Murabayashi, Y.; Abe, M.; Kaga, Y.; Inaba, Y.; Suzuki, M.; et al. Evaluation of novel X-ray protective eyewear in reducing the eye dose to interventional radiology physicians. *J. Radiat. Res.* **2021**, *62*, 414–419. [[CrossRef](#)]
43. Fujibuchi, T. Radiation protection education using virtual reality for the visualisation of scattered distributions during radiological examinations. *J. Radiol. Prot.* **2021**, *41*. [[CrossRef](#)]
44. Kato, M.; Chida, K.; Munehisa, M.; Sato, T.; Inaba, Y.; Suzuki, M.; Zuguchi, M. Non-Lead Protective Aprons for the Protection of Interventional Radiology Physicians from Radiation Exposure in Clinical Settings: An Initial Study. *Diagnostics* **2021**, *11*, 1613. [[CrossRef](#)]
45. Matsubara, K. Assessment of Radiation Dose in Medical Imaging and Interventional Radiology Procedures for Patient and Staff Safety. *Diagnostics* **2021**, *11*, 1116. [[CrossRef](#)]
46. Chida, K.; Inaba, Y.; Morishima, Y.; Taura, M.; Ebata, A.; Yanagawa, I.; Takeda, K.; Zuguchi, M. Comparison of dose at an interventional reference point between the displayed estimated value and measured value. *Radiol. Phys. Technol.* **2011**, *4*, 189–193. [[CrossRef](#)] [[PubMed](#)]
47. International Commission on Radiological Protection (ICRP). *Avoidance of Radiation Injuries from Medical Interventional Procedures*; ICRP Publication 85; Pergamon: Oxford, UK, 2000; Volume 30. Available online: https://journals.sagepub.com/doi/pdf/10.1177/ANIB_30_2 (accessed on 1 November 2022).
48. Haga, Y.; Chida, K.; Kaga, Y.; Sota, M.; Meguro, T.; Zuguchi, M. Occupational eye dose in interventional cardiology procedures. *Sci. Rep.* **2017**, *7*, 569. [[CrossRef](#)] [[PubMed](#)]
49. Kato, M.; Chida, K.; Ishida, T.; Toyoshima, H.; Yoshida, Y.; Yoshioka, S.; Moroi, J.; Kinoshita, T. Occupational radiation exposure of the eye in neurovascular interventional physician. *Radiat. Prot. Dosim.* **2019**, *185*, 151–156. [[CrossRef](#)] [[PubMed](#)]
50. Haga, Y.; Chida, K.; Kimura, Y.; Yamada, S.; Sota, M.; Abe, M.; Kaga, Y.; Meguro, T.; Zuguchi, M. Radiation eye dose to medical staff during respiratory endoscopy under X-ray fluoroscopy. *J. Radiat. Res.* **2020**, *61*, 691–696. [[CrossRef](#)]
51. O'Connor, U.; Walsh, C.; Gallagher, A.; Dowling, A.; Guiney, M.; Ryan, J.M.; McEniff, N.; O'Reilly, G. Occupational radiation dose to eyes from interventional radiology procedures in light of the new eye lens dose limit from the International Commission on Radiological Protection. *Br. J. Radiol.* **2015**, *88*, 20140627. [[CrossRef](#)]
52. Ishii, H.; Haga, Y.; Sota, M.; Inaba, Y.; Chida, K. Performance of the DOSIRIS™ eye lens dosimeter. *J. Radiol. Prot.* **2019**, *39*, N19–N26. [[CrossRef](#)]
53. Ishii, H.; Chida, K.; Satsurai, K.; Haga, Y.; Kaga, Y.; Abe, M.; Inaba, Y.; Zuguchi, M. A phantom study to determine the optimal placement of eye dosimeters on interventional cardiology staff. *Radiat. Prot. Dosim.* **2019**, *185*, 409–413. [[CrossRef](#)]
54. Inaba, Y.; Hitachi, S.; Watanuki, M.; Chida, K. Occupational radiation dose to eye lenses in CT-guided interventions using MDCT-fluoroscopy. *Diagnostics* **2021**, *11*, 646. [[CrossRef](#)]
55. Yashima, S.; Chida, K. Awareness of Medical Radiologic Technologists of Ionizing Radiation and Radiation Protection. *Int. J. Environ. Res. Public Health* **2023**, *20*, 497. [[CrossRef](#)]
56. Martin, C.J.; Magee, J.S. Assessment of eye and body dose for interventional radiologists, cardiologists, and other interventional staff. *J. Radiol. Prot.* **2013**, *33*, 445–460. [[CrossRef](#)]
57. Imai, S.; Akahane, M.; Ogata, Y.; Tanki, N.; Sato, H.; Tameike, K. Occupational eye lens dose in endoscopic retrograde cholangiopancreatography using a dedicated eye lens dosimeter. *J. Radiol. Prot.* **2021**, *41*, 579–589. [[CrossRef](#)]
58. Inaba, Y.; Hitachi, S.; Watanuki, M.; Chida, K. Radiation Eye Dose for Physicians in CT Fluoroscopy-Guided Biopsy. *Tomography* **2022**, *8*, 438–446. [[CrossRef](#)]
59. Inaba, Y.; Nakamura, M.; Chida, K.; Zuguchi, M. Effectiveness of a novel real-time dosimeter in interventional radiology: A comparison of new and old radiation sensors. *Radiol. Phys. Technol.* **2018**, *11*, 445–450. [[CrossRef](#)]
60. Chida, K.; Kato, M.; Inaba, Y.; Kobayashi, R.; Nakamura, M.; Abe, Y.; Zuguchi, M. Real-time patient radiation dosimeter for use in interventional radiology. *Phys. Med.* **2016**, *32*, 1475–1478. [[CrossRef](#)]
61. Haskal, Z.J.; Worgul, B.V. 2004 Interventional radiology carries occupational risk for cataracts. *RSNA News.* **2004**, *14*, 5–6.
62. Ainsbury, E.A.; Bouffler, S.D.; Dörr, W.; Graw, J.; Muirhead, C.R.; Edwards, A.A.; Cooper, J. Radiation cataractogenesis: A review of recent studies. *Radiat. Res.* **2009**, *172*, 1–9. [[CrossRef](#)]
63. Nakamura, M.; Chida, K.; Zuguchi, M. Novel Dosimeter Using a Nontoxic Phosphor for Real-Time Monitoring of Patient Radiation Dose in Interventional Radiology. *AJR Am. J. Roentgenol.* **2015**, *205*, W202–W206. [[CrossRef](#)]
64. Nakamura, M.; Chida, K.; Zuguchi, M. Red emission phosphor for real-time skin dosimeter for fluoroscopy and interventional radiology. *Med. Phys.* **2014**, *41*, 101913. [[CrossRef](#)]
65. Diagnostic Reference Level in Japan (2020 Version). Available online: http://www.radher.jp/J-RIME/report/JapanDRL2020_jp.pdf (accessed on 1 November 2022).

Disclaimer/Publisher's Note: The statements, opinions and data contained in all publications are solely those of the individual author(s) and contributor(s) and not of MDPI and/or the editor(s). MDPI and/or the editor(s) disclaim responsibility for any injury to people or property resulting from any ideas, methods, instructions or products referred to in the content.